

Article

Improving center vortex detection by usage of center regions as guidance for the direct maximal center gauge

Rudolf Golubich ¹ , Manfred Faber * 

¹ Atominstitut, Techn. Univ. Wien; rudolf.golubich@gmail.com

* Atominstitut, Techn. Univ. Wien; faber@kph.tuwien.ac.at

Abstract: The *center vortex model* of quantum chromodynamic states that vortices, closed color-magnetic flux, percolate the vacuum. Vortices are seen as the relevant excitations of the vacuum, causing confinement and dynamical chiral symmetry breaking. In an appropriate gauge, as *direct maximal center gauge*, vortices are detected by projecting onto the center degrees of freedom. Such gauges suffer from Gribov copy problems: different local maxima of the corresponding gauge functional can result in different predictions of the string tension. By using non-trivial center regions, that is, regions whose boundary evaluates to a non-trivial center element, a resolution of this issue seems possible. We use such non-trivial center regions to guide simulated annealing procedures, preventing an underestimation of the string tension in order to resolve the Gribov copy problem.

Keywords: quantum chromodynamics; confinement; center vortex model; string tension; Gribov copy problem

PACS: 11.15.Ha, 12.38.Gc

0. Introduction

First proposed by 't Hooft [1] and Cornwall [2] the *center vortex model* gives an explanation of confinement in non-abelian gauge theories. It states that the vacuum is a condensate of quantised magnetic flux tubes, the so called *vortices*. The vortex model is able to explain:

- behaviour of Wilson loops, see [3],
- finite temperature phase transition \rightarrow Polyakov loops,
- orders of phase transitions in SU(2) and SU(3),
- Casimir scaling of heavy-quark potential, see [4],
- spontaneous breaking of scale invariance, see [5],
- chiral symmetry breaking, see [6,7] \rightarrow quark condensate,

but suffers from Gribov copy problems: predictions concerning the string tension depend on the specific implementation of the gauge fixing procedure, see [8,9].

In this work, an explanation of the problem is given before an improvement of the vortex detection is presented.

Center vortices are located by P-vortices, which are identified in direct maximal center gauge, the gauge which maximizes the functional

$$R^2 = \sum_x \sum_\mu | \text{Tr}[U_\mu(x)] |^2. \quad (1)$$

The projection onto the center degrees of freedom

$$Z_\mu(x) = \text{sign Tr}[U_\mu(x)]. \quad (2)$$

27 leads to plaquettes with non-trivial center values, P-plaquettes which form P-vortices, closed surfaces
 28 in dual space. This procedure can be seen as a best fit procedure of a thin vortex configuration to a
 given field configuration [3,10], see Figure 1. That P-vortices locate thick vortices is called *vortex finding*

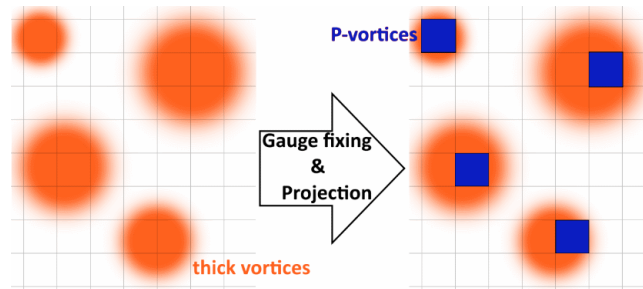


Figure 1. Vortex detection as a best fit procedure of P-Vortices to thick vortices shown in a two dimensional slice through a four dimensional lattice.

29
 30 *property.*

Center vortices can be directly related to the string tension: the flux building up the vortex contributes a non-trivial center element to surrounding Wilson loops, see Figure 2. The behaviour of

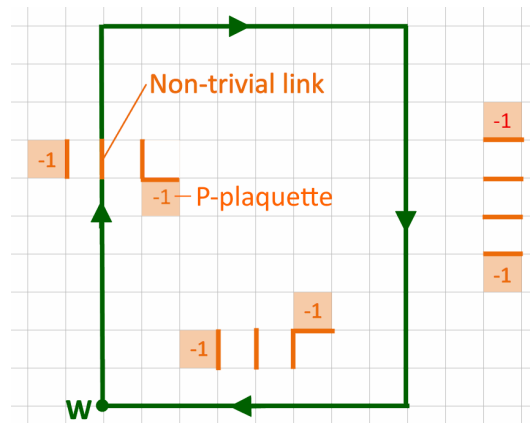


Figure 2. Each P-plaquette contributes a non-trivial center element to surrounding Wilson loops.

Wilson loops can be explained and a non vanishing string tension extracted by using the density ρ_u of uncorrelated P-plaquettes per unit volume

$$\langle \frac{1}{2} \text{Tr}(\mathbf{W}(R, T)) \rangle = [-1 \rho_u + 1 (1 - \rho_u)]^{R \times T} = e^{\ln(1-2\rho_u) R \times T} \Rightarrow \sigma = -\ln(1 - 2 \rho_u). \quad (3)$$

The string tension can also be calculated by Creutz ratios

$$\chi(R, T) = -\ln \frac{\langle \mathbf{W}(R+1, T+1) \rangle \langle \mathbf{W}(R, T) \rangle}{\langle \mathbf{W}(R, T+1) \rangle \langle \mathbf{W}(R+1, T) \rangle}. \quad (4)$$

31 From $\langle \mathbf{W}(R, T) \rangle \approx e^{-\sigma R T - 2 \mu (R+T) + C}$ follows for sufficiently large R and T that $\chi(R, T) \approx \sigma$. Creutz
 32 ratios for center projected Wilson loops are expected to give correct values for σ if the vortex finding
 33 property is given.

34 The problem with the direct maximal center gauge is that different local maxima of the gauge
 35 functional R can lead to different predictions concerning the string tension in center projected
 36 configurations [8,9]. An improvement in the value of the gauge functional results in an underestimation
 of the string tension as can be seen in Figure 3. In fact, preliminary analysis show that the string tension

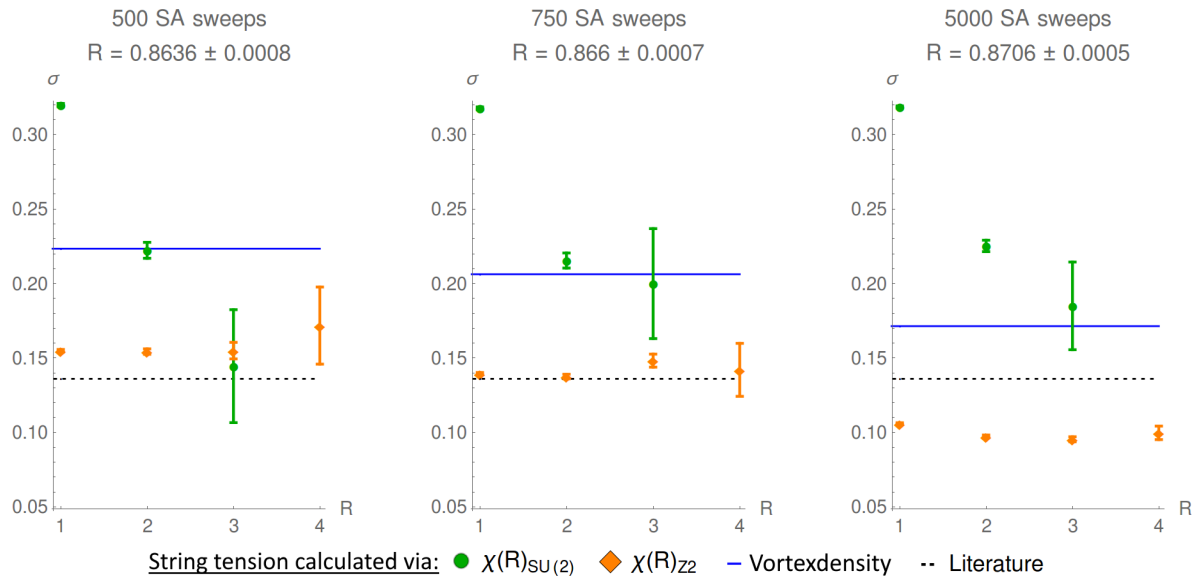


Figure 3. The string tension, calculated via Creutz ratios of the full theory $\chi(R)_{SU(2)}$, the center projected theory $\chi(R)_{Z2}$ and the vortex density. By increasing the number of simulated annealing sweeps a better value of gauge functional is reached, but the string tension underestimated by $\chi(R)_{Z2}$. The data was calculated in lattices of size 12^4 (left), 12^4 (middle) and 14^4 (right) in Wilson action. The vortex density was not corrected for correlated P-plaquettes, hence is overestimated.

37 decreases linearly with an improvement in the value of the gauge functional.

38 We believe that this is caused by a failing gauge fixing procedure during which the vortex finding
 39 property is lost. If the P-vortices fail to locate thick vortices the string tension will be underestimated
 40 by $\chi(R)_{Z2}$, see Figure 4. A failing vortex detection can result in vortex clusters disintegrating into small

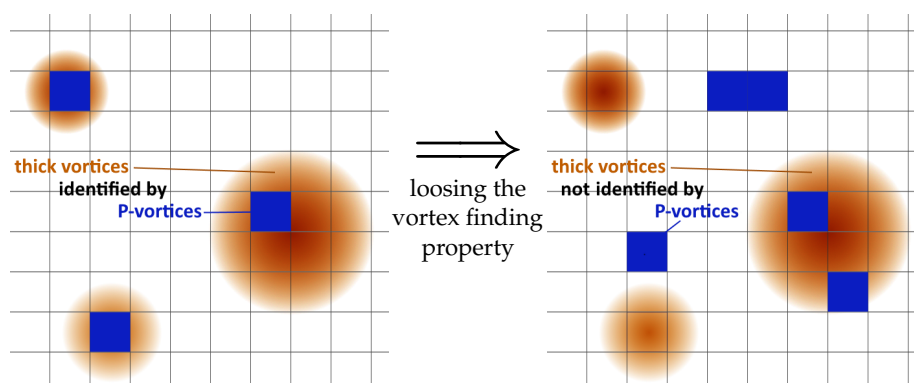


Figure 4. When P-vortices no longer locate thick vortices, we speak of a loss of the *vortex finding property*. The figure shows a two dimensional slice through a four dimensional lattice.

41 vortices consisting only of correlated P-plaquettes. This causes a misleadingly high vortex density.

42 The loss of the vortex finding property can be avoided by using the information about center
 43 regions, that is, regions, enclosed by a Wilson loop that evaluate to center elements.
 44

Center regions can be related to a non-Abelian generalization of the Abelian Stokes theorem:

$$P \exp \left(i \oint_{\partial S} A_\mu(x) dx^\mu \right) = \mathcal{P} \exp \left(\frac{i}{2} \int_S \mathcal{F}_{\mu\nu}(x) dx^\mu dx^\nu \right), \quad (5)$$

$$\mathcal{F}_{\mu\nu}(x) = U^{-1}(x, O) F_{\mu\nu}(x) U(x, O), \quad U(x, O) = P \exp \left(i \int_l A_\eta(y) dy^\eta \right),$$

45 with P denoting path ordering, \mathcal{P} "surface ordering" and l being a path from the base O of ∂S to x , see
 46 [11]. The left hand side of (5) can be identified as the evaluation of a Wilson loop spanning the surface
 47 S . The right hand side can be expressed using plaquettes: $U_{\mu\nu}(x) = \exp (ia^2 F_{\mu\nu} + \mathcal{O}(a^3))$, with lattice
 48 spacing a , see [12]. With this ingredients the non-Abelian Stokes theorem reads in the lattice as is
 shown in Figure 5:

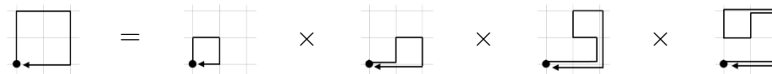


Figure 5. Factoring a Wilson into factors of plaquettes using the non-Abelian Stokes theorem.

49 By finding center regions, that is, plaquettes within S that combine to bigger regions which
 50 evaluate to center elements, the Wilson loop spanning S can be factorized into a commuting factor, a
 51 center element, and an non-Abelian part, see figure 6.

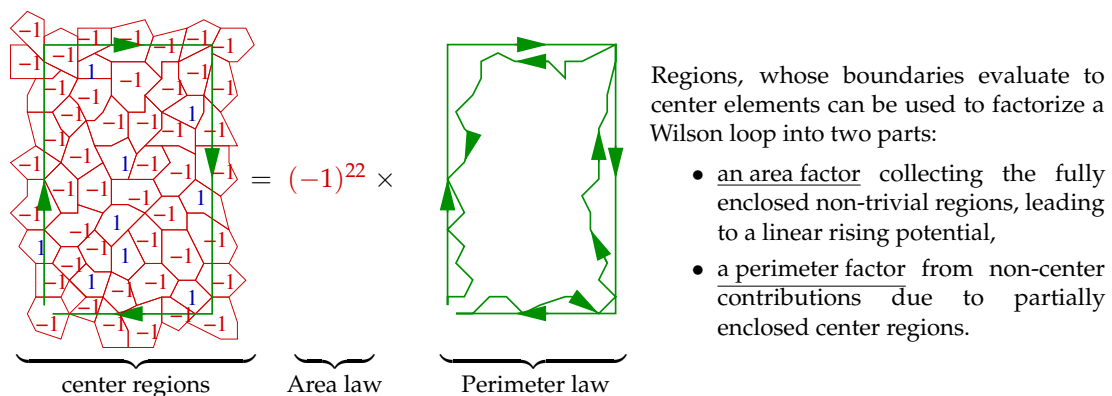


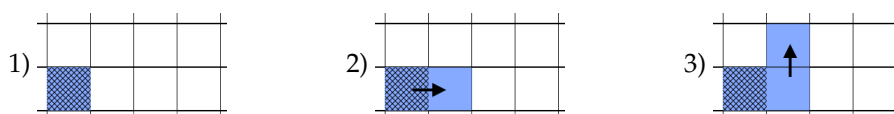
Figure 6. Center regions explain the coulombic behaviour and the linear rise of the quark anti-quark potential as they lead to an area law and a perimeter law for Wilson loops.

52 The center regions capture the center degrees of freedom and can be directly related to the
 53 behaviour of Wilson loops. It seems reasonable to demand that their evaluation should not be changed
 54 by center gauge or projection on the center degrees of freedom. We show that by preserving non-trivial
 55 center regions the loss of the vortex finding property is prevented and the full string tension can be
 56 recovered.
 57

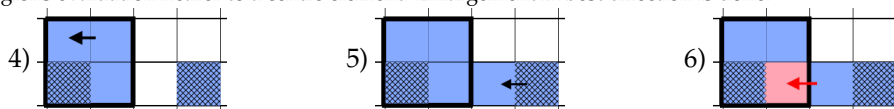
58 1. Materials and Methods

59 The predictions of the center vortex model concerning the string tension in SU(2) gluonic quantum
60 chromodynamic are analysed by calculating the Creutz ratios after center projection in maximal
61 center gauge. The gauge fixing procedure is based upon simulated annealing, maximizing the
62 functional (1), that is, bringing each link as close to an center element as possible. The simulated
63 annealing algorithms are modified, so that the evaluation of center regions is preserved during the
64 procedure: transformations resulting in non-trivial center regions projecting onto the non-trivial center
65 element are enforced and transformations resulting in non-trivial center regions projecting onto the
66 trivial center element are prevented.

67 The detection of the non-trivial center regions of one lattice configuration is done by enlarging
68 regions until their evaluation becomes nearest possible to a non-trivial center element, see Figure 7.
The algorithm starts with sorting the plaquettes of a given configuration by rising trace of their



Steps 1-3: Starting with a plaquette that neither belongs to an already identified centre region, nor has already been taken as origin for growing a region, it is tested, which enlargement around a neighbouring plaquette brings the regions evaluation nearer to a centre element. Enlargement in best direction is done.



Steps 4-6: If no enlargement leads to further improvement, a new enlargement procedure is started with another plaquette. While its enlargement it can happen, that it would grow into an existing region. The collision handling described in following is used to prevent this:



Step 7a: The evaluation of the growing region is nearer to a non-trivial centre element than the evaluation of the old region: Delete the old region, only keeping the mark on its starting plaquette and allow growing.

Step 7b: The growing region evaluates further away from a non-trivial centre element than the existing one: prevent growing in this direction and, if possible, enlarge in second best direction instead. Multiple collisions after growing are possible.

Figure 7. The algorithm for detecting centre regions repeats these procedures until every plaquette either belongs to an identified region or has been taken once as starting plaquette for growing a region. The arrow marks the direction of enlargement. Plaquettes belonging to a region are coloured, plaquettes already used as origin are shaded.

69 evaluation. This stack is worked down plaquette by plaquette, enlarging each as far as possible by
70 adding neighbouring plaquettes. During this procedure, collisions of growing regions are prevented.

71 The regions identified this way comprise also many, whose evaluation deviates far from the
72 center of the group. A set of non-trivial center regions has to be selected from the set of identified
73 regions: Only regions with traces smaller then Tr_{\max} are taken into account. This parameter Tr_{\max} has
74 to be adjusted under consideration of the behaviour of Creutz ratios as shown in Figure 8 which are
75 calculated after gauge fixing and center projection.

76 At low values of Tr_{\max} the Creutz ratios are expected to be nearly constant with respect to the
77 loop size. With raising Tr_{\max} they start to approach their asymptotic value from above and become
78 chaotic with Tr_{\max} chosen inappropriately high.

79 As the center degrees of freedom are expected to capture the long range behaviour, the Creutz
80 ratios calculated in center projected configurations are near to the correct value of the string tension
81 already for small loop sizes. Hence we chose Tr_{\max} as high as possible without causing the behaviour
82 of the Creutz ratios to approach the string tension from above.
83

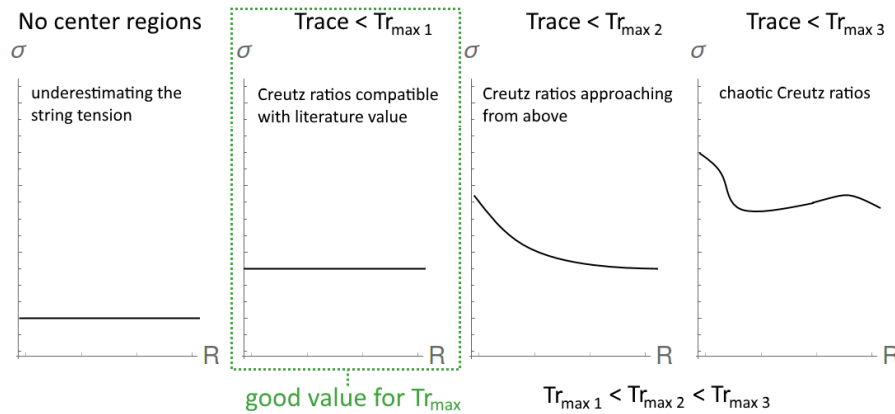


Figure 8. Tr_{\max} can be fine tuned by looking at the dependency of the Creutz ratios on the loop size R .

84 The regions determined by this procedure are then used to guide the gauge fixing procedure. The
 85 influence on the predicted string tension is analysed by calculating the Creutz ratios in center projected
 86 configurations.

87 2. Results

88 Here we present the calculations of the center vortex string tension for different values of Tr_{\max}
 89 at $\beta = 2.3$. Similar results were obtained for $\beta = 2.4$ and $\beta = 2.5$. In the following, only the Creutz
 90 ratios of the center projected configurations $\chi(R)_{Z2}$ are of relevance. The Creutz ratios of the full $SU(2)$
 91 theory $\chi(R)_{SU(2)}$ and the calculations of the string tension based on the vortex density are calculated
 92 for comparison. They are only shown for the sake of completeness. All data was calculated with $SU(2)$
 93 Wilson action.

94 The Creutz ratios tend towards the literature value of the string tension with increasing number
 95 of simulated annealing steps with a $Tr_{\max} = -0.985$, whereas they clearly underestimate the string
 tension when center regions are ignored, see Figure 9. The full string tension can be easily recovered,

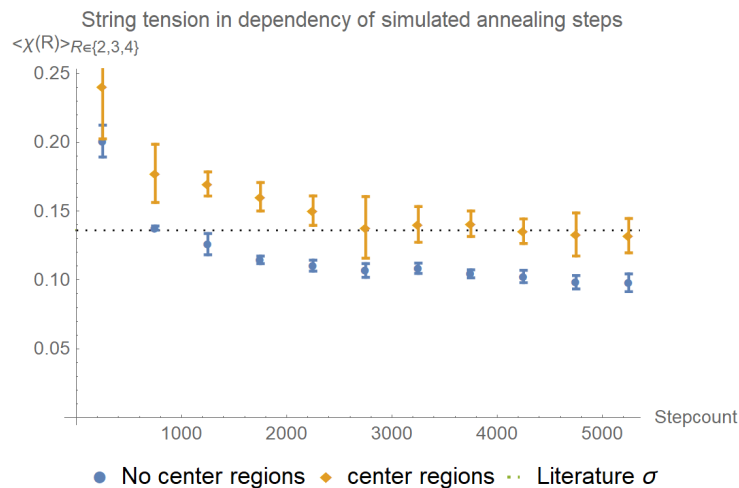


Figure 9. By preserving center regions the Creutz ratios tend towards the literature value of string tension during the simulated annealing procedure. The data was calculated at $\beta = 2.3$ in an 12^4 lattice with 100 configurations taken into account per datapoint. Displayed is the mean of $\chi(2)$, $\chi(3)$ and $\chi(4)$. The increased error bars when center regions are preserved might be because the algorithm does not reach the exact local maxima, but fluctuates around it.

96 although the value of the gauge functional is reduced, see Figure 10. The upper three graphs show the
 97 calculations done for optimizing the value of Tr_{\max} . The final results, shown in the left graph in the
 98

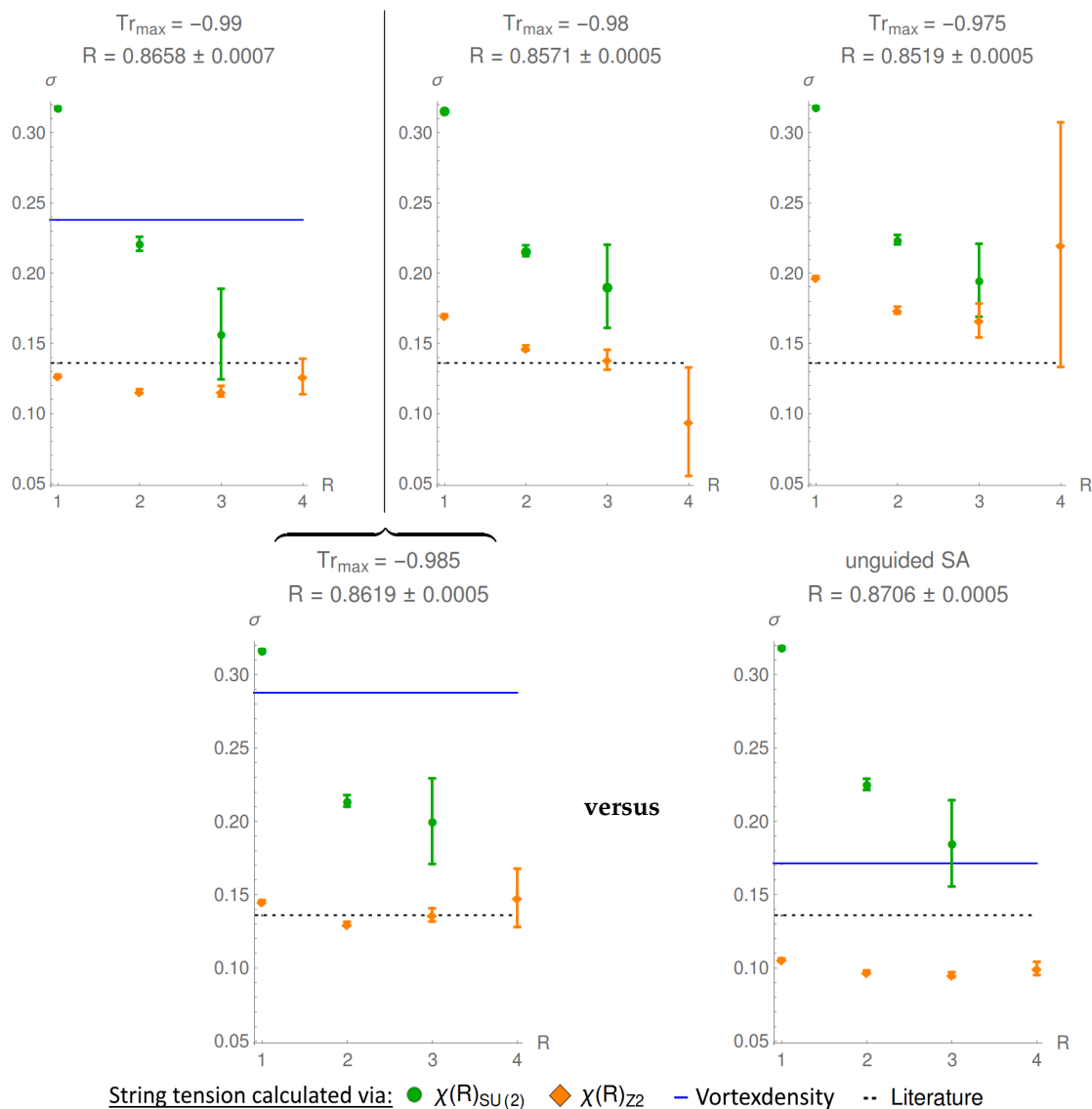


Figure 10. Optimization of Tr_{max} in the upper line and final results for the guided simulated annealing in the lower row at $\beta = 2.3$. The creutz ratios were calculated with 300 Wilson configurations at $\beta = 2.3$ in lattices of sizes 12^4 in the upper left graph and 14^4 for the other graphs. The error bars are calculated with the one-deletion-Jackknife method. The optimal value of Tr_{max} was identified by taking into account the behaviour of the Creutz ratios and found to be around $Tr_{\text{max}} \approx -0.985$, reducing the value of gauge functional from $R = 0.871$ to $R = 0.862$.

99 lower row are calculated with a value of $Tr_{\text{max}} = -0.985$, that is, a value between the respective values
 100 of the left and middle graph in the upper line. The final results are compared with raw simulated
 101 annealing, that is, without preserving center regions shown in the right graph of the lower row. The
 102 large errors using center regions might result from fluctuations of the gauge functional around the
 103 maxima which can not be reached due to the constraint of the preservation of center regions: further
 104 approaches to the local maxima of the gauge functional are therefore prevented.

105 3. Discussion

106 By preserving non-trivial center regions the full string tension can be recovered and extracted from
107 the center degrees of freedom in SU(2) quantum chromodynamics. The choice of the free parameter
108 Tr_{\max} based on the behaviour of Creutz ratios does not give an unambiguous value, but merely an
109 interval of good values of Tr_{\max} . This arbitrariness has to be investigated in further work. Preliminary
110 data already hints at a way to eliminate it. The concept of identifying gauge independent observables
111 evaluating to the relevant degrees of freedom and using them to guide the gauge fixing procedure
112 reduces the number of free parameters of the gauge transformation. It forces all differing local maxima
113 of the gauge functional to incorporate specific, gauge invariant properties that are related to the
114 relevant degrees of freedom. This might be a solution to the Gribov copy problem wherever the gauge
115 fixing procedure is based upon a specific gauge functional. The algorithms presented can be easily
116 extended into higher symmetry groups or modified to capture different degrees of freedom. The
117 procedures for identifying non-trivial center regions can also be used to reconstruct the thick vortices
118 from P-plaquettes. This will allow further investigations of the color structure of vortices.

119 **Acknowledgments:** We thank Vitaly Bornyakov for the helpful discussions of the results.

120 References

- 121 1. 't Hooft, G. On the phase transition towards permanent quark confinement. *Nuclear Physics B* **1978**, *138*, 1 –
122 25. doi:[https://doi.org/10.1016/0550-3213\(78\)90153-0](https://doi.org/10.1016/0550-3213(78)90153-0).
- 123 2. Cornwall, J.M. Quark confinement and vortices in massive gauge-invariant QCD. *Nuclear Physics B* **1979**,
124 *157*, 392 – 412. doi:[https://doi.org/10.1016/0550-3213\(79\)90111-1](https://doi.org/10.1016/0550-3213(79)90111-1).
- 125 3. Del Debbio, L.; Faber, M.; Giedt, J.; Greensite, J.; Olejnik, S. Detection of center vortices in
126 the lattice Yang-Mills vacuum. *Phys. Rev.* **1998**, *D58*, 094501, [[arXiv:hep-lat/9801027](https://arxiv.org/abs/hep-lat/9801027)].
127 doi:10.1103/PhysRevD.58.094501.
- 128 4. Faber, M.; Greensite, J.; Olejnik, S. Casimir scaling from center vortices: Towards an understanding
129 of the adjoint string tension. *Phys. Rev.* **1998**, *D57*, 2603–2609, [[arXiv:hep-lat/9710039](https://arxiv.org/abs/hep-lat/9710039)].
130 doi:10.1103/PhysRevD.57.2603.
- 131 5. Langfeld, K.; Reinhardt, H.; Tennert, O. Confinement and scaling of the vortex vacuum of
132 SU(2) lattice gauge theory. *Phys. Lett.* **1998**, *B419*, 317–321, [[arXiv:hep-lat/9710068](https://arxiv.org/abs/hep-lat/9710068)].
133 doi:10.1016/S0370-2693(97)01435-4.
- 134 6. Höllwieser, R.; Schweigler, T.; Faber, M.; Heller, U.M. Center Vortices and Chiral Symmetry
135 Breaking in SU(2) Lattice Gauge Theory. *Phys. Rev.* **2013**, *D88*, 114505, [[arXiv:hep-lat/1304.1277](https://arxiv.org/abs/hep-lat/1304.1277)].
136 doi:10.1103/PhysRevD.88.114505.
- 137 7. Faber, M.; Höllwieser, R. Chiral symmetry breaking on the lattice. *Prog. Part. Nucl. Phys.* **2017**, *97*, 312–355.
138 doi:10.1016/j.pnpnp.2017.08.001.
- 139 8. Bornyakov, V.G.; Komarov, D.A.; Polikarpov, M.I.; Veselov, A.I. P vortices, nexuses and effects of
140 Gribov copies in the center gauges. Quantum chromodynamics and color confinement. Proceedings,
141 International Symposium, Confinement 2000, Osaka, Japan, March 7-10, 2000, 2002, pp. 133–140,
142 [[arXiv:hep-lat/0210047](https://arxiv.org/abs/hep-lat/0210047)].
- 143 9. Faber, M.; Greensite, J.; Olejnik, S. Remarks on the Gribov problem in direct maximal center gauge. *Phys.*
144 *Rev.* **2001**, *D64*, 034511, [[arXiv:hep-lat/0103030](https://arxiv.org/abs/hep-lat/0103030)]. doi:10.1103/PhysRevD.64.034511.
- 145 10. Faber, M.; Greensite, J.; Olejnik, S. Direct Laplacian center gauge. *JHEP* **2001**, *11*, 053,
146 [[arXiv:hep-lat/0106017](https://arxiv.org/abs/hep-lat/0106017)]. doi:10.1088/1126-6708/2001/11/053.
- 147 11. Broda, B. NonAbelian Stokes theorem **1995**. pp. 496–505, [[arXiv:hep-th/9511150](https://arxiv.org/abs/hep-th/9511150)].
- 148 12. Gattringer, C.; Lang, C. *Quantum Chromodynamics on the Lattice: An Introductory*; Springer-Verlag, 2010.

149 **Sample Availability:** All data and Fortran source codes of the algorithms are available from the authors.